

Utilizing Stress Transmissions in Bonded Granular Materials to Determine Grain Contact Stiffness in Sandstone

A. G. Olugbenga and S. J. Antony

Abstract—An experimental investigation of stress transmission through bonded particulate structures with visible stress pattern and stress-strain data from rock matrix akin to the problem of rock fracturing remains a challenge and this is addressed in the present work. The stress transmission through sandstone under mechanical loading is analyzed experimentally by applying a thin coating of birefringent material. The retardation of the light components that reflect from the surface of the birefringent on sandstone samples was measured. By using a reflection type optical tomography, the maximum shear stress under the external loading indicates stressed point on the surface of the sample which was related to grain displacement. The strain induced birefringence occurs due to the anisotropy within the grains in the sandstone which result isochromatic fringes. Hence the shear stress map on the surface of the sandstone sample was visualized. This information is used further to evaluate modulus at micro scale and the yield strength. The stress measurement made from photo-stress experimental techniques was compared with the ultrasound sensors, strain gauges and bulk strength devices. Analogous to this experiment, simulations using Discrete Element Modeling (DEM) were performed using the measured grain-scale parameters as inputs. The boundary and initial conditions for the experimental conditions were used to simulate force distribution for sandstone under compression. The stiffness ratio associated with the grain-to-grain cementation in experiment agrees excellently with the simulations. This makes it possible to visualize and understand how micro-scale behavior contributes to the bulk strength characteristics of cementations in materials even when they are opaque.

Index Terms—Bonded particles, granular assembly, anisotropy, birefringence, stiffness ratio

I. INTRODUCTION

QUALITATIVE approaches to probing strength characteristics of strongly bonded (rock-like) particulate materials has been attempted in the past; [1], [2] and [3]. However the concept of accounting grain scale interactions within grains bonded with cement-like structure such as rock and concrete is not sufficiently developed for formulating contact models for the materials. Therefore, a

more significant step to understand the behavior of strength of sandstone is presented in this work where the stress distribution on opaque sandstone under mechanical loading using photo stress analysis tomography (PSAT) was obtained. In this, stress-sensitive thin coating was initially applied on the sandstone which is sufficiently free of residual-stress and adherent on rock surface. Using reflective type PSAT [4], shear stress distribution on the sample can be visualized during external loading. From this, examinations are performed to derive the contact stiffness parameters suitable for feeding into their DEM simulations. Further the contact parameter was validated with the P-wave and S-wave data using ultrasound probes. The Qua ibo sandstone (with grain size 80-100 microns) was used in this study.

The particle flow code have been employed to obtain the macro-parameters of rock by first defining calibration as micro parameters. Micro properties of sandstone can be made to interact to produce corresponding macro properties of the material. Further the macro properties are then synthesized to produce the material behavior under stress. The work of [5] have shown that the choice of appropriate micro parameters depends largely on the material behavior. The particles are simulated as bonded together with cement called parallel bond where they closely interact by contact forces occurring in every particle to particle contact point. The degree of closeness of the particles makes the packing properties cohesive but the bonded particles are connected by parallel bond. The bond is a finite dimensionally equal to the particle diameter [6]. It possesses both tensile and shears strength, the stiffness of both normal and tangential strength. The external application of load leads to stress transmission in the material, when either of the strength are exceeded, the parallel bond breaks and forms micro-cracks inside the rock mass between the particles. Coalescence of the micro-cracks occurs as the loading weight increases which are seen as cracks which divide the rock mass into separate clusters. The location of this failure point can be tracked from the onset by accurate evaluation of both contact and parallel bond existing in the microstructure of the material. In this work the micro-mechanical properties are estimated experimentally and simulated and are presented for the evaluation and determination of deformability of rock material.

Manuscript received March 23, 2021; revised April 08, 2021.

A. G. Olugbenga is a Senior Lecturer of the Department of Chemical Engineering of Federal University of Technology Minna, Nigeria PMB 65 Minna phone: +234-906-3533503; e-mail: grace.adeola@futminna.edu.ng.

S. J. Antony is an Associate Professor of School of Chemical and Process Engineering University of Leeds, LS2 9JT. UK. Phone: +44(0)113 343 2409 e-mail: s.j.antony@leeds.ac.uk

II. EXPERIMENTAL AND NUMERICAL METHODOLOGY

A. Determination of Contact Parameters

Reflective PSAT methodology (Fig. 1 and 2) is used to map out the shear stress profile on the chosen V-notch samples under the external loading. More details on its working principle can be found elsewhere [7]. Using this, the stiffness parameters (normal and shear) were obtained from the extracted data for fringe order and the force applied to induce stress into the material. The geometry of the sample was the modified short rod test [8].

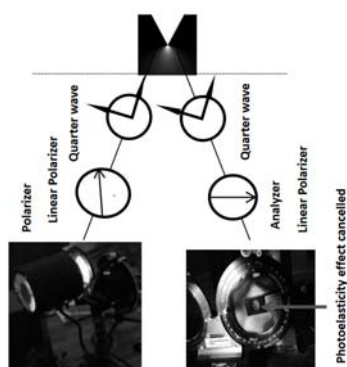


Fig. 1. Experimental Set up for PSAT.

B. Determination of Poisson's Ratio and Grain Contact Stiffness from P-wave and S-wave measurements

The sensors were placed at the top and bottom of the rock sample which were subjected to compressional loading. The sensors were linked to ultrasonic digital indicator which consist, transmitter, a pulse generator unit and the receiver transducers were used for sonic pulse velocity measurement. The wave travel time was measured. The velocity was calculated from dividing the length of rock sample by wave travel time. Both the P-wave and the S-wave velocities were measured. The modified Digby's equation provided by [1] was used to obtain normal stiffness and tangential stiffness of the grain contact. The corresponding experimental macroscopic data for elastic modulus and Poisson's ratio were determined.

C. Mathematical Modeling of Contact Behavior of Sandstone

The study of contact behavior was carried out using DEM. In order to set up a model with DEM [6], three fundamental components obtained from micro strain measurement from sandstone were specified; an assembly of particles, contact behavior and material properties, the boundary and initial conditions were included.

III. RESULTS AND DISCUSSION

A. Contact Behavior and Material Properties for Description of Force Transmission

The physical behavior occurring at a contact is explained in this work using linear contact model [6] with shear and normal bond stiffness. Cement-like material may exhibit a nonlinear behavior which is complex to understand. This is because the inherent structural bonding and arrangement of the grains could be more anisotropic in the natural

sandstone samples than normally simulated in computational studies [9]. In the current experiments, as the stress profiles are obtained on the actual samples, the anisotropy in the structural arrangement of the grains is automatically accounted for. In this study the contact model is described in terms of three types of interaction characteristics: (1) a contact stiffness model; (2) a slip and separation model; and (3) a bonding model.

B. Contact Stiffness Model, Slip and Bond Model

Fig. 2 shows the typical images of maximum shear stress contours observed under different load levels. Also Figure 3 presents the experimentally measured results for the tension and compressional stiffness data from the photo fringe data for the sandstone, which has a slope ratio of 2.4 between them. Hence, the ratio of the contact normal to shear stiffness is observed as 2.4 (Fig. 3) for the sandstone sample. This data will form as input to the DEM modeling.

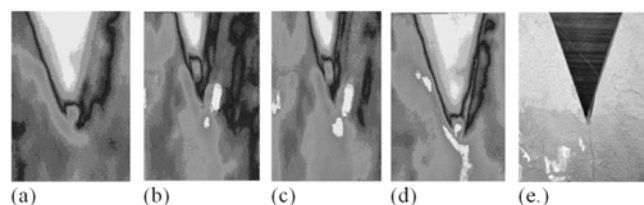
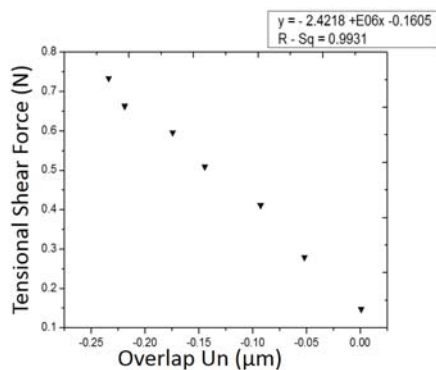
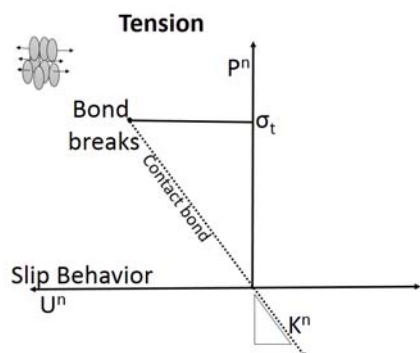


Fig. 2. Contours of Maximum Shear Stress Distribution for (a)70KN (b)80KN (c)100KN and (d) 120KN Load (e) Natural sandstone cracked at the line of maximum stress location for PSAT.

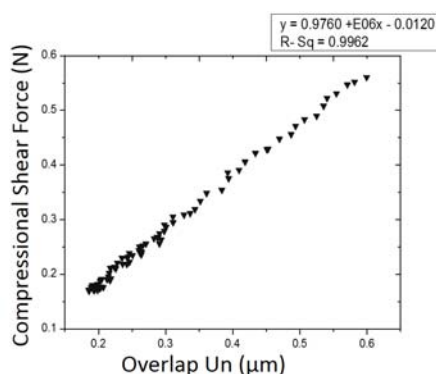
When light passes through a medium, it can be refracted. This phenomenon is governed by Snell's law similar to the ultrasound technique. The light is refracted when the medium of transmission changes. The refracted light is plane polarized. But when only a single ray of light passes through the medium, it is refracted. When sandstone sample was subjected to loading, the strain in the rock was transferred to the coated surface which exhibits an optical anisotropic property (called birefringence). A single ray is refracted which produce two refracted rays. Fig. 2 shows the fringe pattern that was observed and the crack pattern in the trace of maximum stress. Tension data was recorded before the compression region is approached (Fig. 3c and d), but in (Fig. 2) only the maroon fringe (represented as grey) indicating the compression is presented. The fringe begins to expand out as the grain contact bonds continue to deform until a critical shear stress is reached where the bond breaks (representing white thick line in Fig. 2a-d). Each grain is displaced relative to another neighboring grain characterizing the slip behavior of the grain as a positive overlap. The negative trend observed in the tension region (Fig. 3a) is due to direction of grains which is normal in tension. Hence the bond breakage precedes the grain displacement (Fig. 3b). This is true to support the theory provided by linear model for a contact between particles [5] [10] adopted their research work based on this principle too.



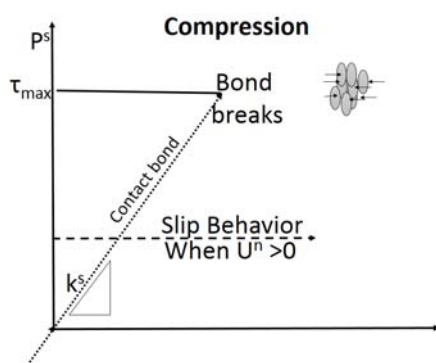
(a)



(b.)



(c.)



(d.)

Fig. 3. (a) Tensional shear force plot (b.) compressional shear force (c.) illustration of the bond breakage in tension (d.) illustration of the bond breakage in compression

C. Combined Approach between Photo Stress Analysis and Discrete Modeling

The shear strain and shear stress data were the point data

extracted from the experiments; it was plotted and the slope of the linear region was assigned grain modulus or bond modulus.

Each grain of the granular assembly of the sandstone are sand-sized (1/16 to 2 mm diameter) of the detrital fragments [11] and [12]. These grains are called quartz framework grains which are the dominate minerals in most sedimentary rocks. The hardness and chemical stability allow the quartz grains to display some degree of roundness [13]. For this evaluation, $6.25 \times 10^{-5} \text{m}$ was taken as the particle radius. Subsequently the grain stiffness ratio was established to be 2.4 by evaluating the ratio of the two slopes in Fig. 3a and 3c

D. Comparison of PSAT Technique with the Ultrasound Experiments

A wave is refracted when ultrasound wave passes through an interface or micro-defect in rock matrix [14]. The same phenomenon occurs when light passes through an interface. Refraction occurs in rock because of the velocity difference between the gel medium and the rock medium [15]. The larger the difference in the acoustic properties of the two media, the greater the refraction produced. The angle of incidence at which the sound wave enters the rock and their velocities can be correlated. This correlation is called Snell's law. By this technique, both shear and longitudinal wave are refracted. The reflective beam for longitudinal and shear waves were as discussed in the PSAT technique.

It is known that texture property (e.g. the grain to grain contact, the grain spherical index, sorting and bonding) of the rock could influence on the wave propagation velocities through the rock matrix [16]. These properties control the wave propagation through the rock. [17] It was observed that poorly connected grain to grain contacts are much more likely to reduce the wave velocities, because larger grains have larger contact length within the grain assembly. Therefore ultrasound experiments are used in this research to measure the P-wave and S-wave velocities that pass through the sandstone. The average of the velocity ratio averaged was 1.53. This was used in Digby's equation to evaluate the stiffness ratio [1] which results a value of 2.28. Thus the value of the stiffness ratio for ultrasound is within the range of the outcome from the PSAT experiments.

E. An assembly of particles

For the DEM modeling, the bond modulus is 13GPa, the stiffness ratio is 2.4 and the grain diameter was in the range of 80 -100microns. The tensile strength is 3MPa for the model dimensions of 5 by 10 by 5mm, normally, the contact behavior and associated material properties dictate the type of response the model will display during deformation.

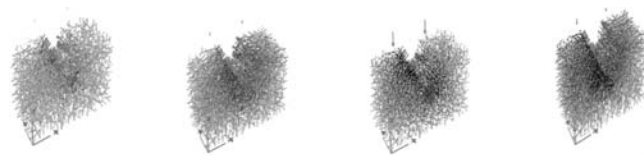
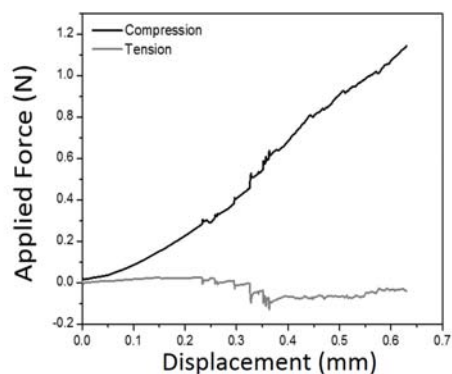
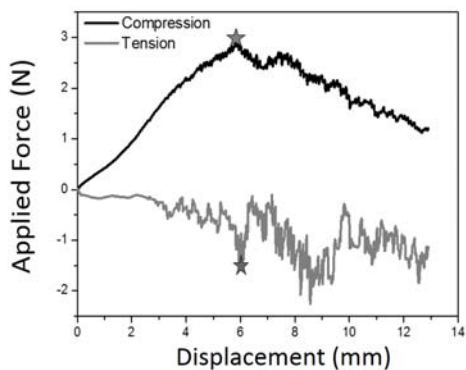


Fig. 4. Force chains of stress transmission during loading at 0.4N, 0.8N, 1N and 2N. The lighter colored force chains are compression while dark colored force chains are tension



(a.)



(b)

Fig. 5. For DEM (a.) contact force displacement of tension and compression (before bond rupture with displacement at 0.5mm) (b.) Stress-displacement behavior at particle contact before 12mm displacement

The boundary and initial conditions were defined for in-situ state of the sample with the V-notch similar to the samples used in the experiments. After these conditions were defined, the initial equilibrium state was attained for the model. The resulting response of the model was reached under different axial load levels. The stress transmission was tracked beneath the notch at load level 0.4N, 0.8N, 1N and 2N (Fig. 4). A. Particle Contact Force, Tension and Compressive Response of Sandstone. The lower curve shows that the force data becomes increasingly negative until the highest possible negative force is reached. Fig. 4 shows the force chains at 0.4N to 2N. The corresponding graph of grain contact displacement is plotted in Fig. 5. The first highest point of negativity has been described to be the point of bond rupture in tension. This is in agreement with the reference of [18]. It is also important to note that the tensile behavior occurs at the initial loading stages. Thus the force load that corresponds to the tensile strength is about 2MPa. The negative value is due to direction. The force measurement during the compression on force chain shows that the compressive data becomes increasingly positive until the bond fail under compression (Fig. 5b). The force at 2.4N is the yield strength of a contact bond at which bond ruptures. The compression exerted on the contact force chain that link particles reduce the bond strength at grain contact. Hence micro-fracture is formed and the crack nucleation occurs. In this test, grain contact bond breaks at 2.4MPa (Fig. 5b). During the crack propagation represented by the coalescence of multiple rupture of contact bond, particles rotate as a representation of final shearing away from the contact. In Fig. 5b, however, the moment resulting

from two contacting particle rotation is opposed by the surrounding elastic spring connecting other neighboring particles. This network of force chain is distorted and the materials become deformed. The shearing is not uniform (Fig. 5b). In order to make the macro-parameter of the simulated rock to be the same as the obtained value from the physical experiments, micro parameter values were chosen by trial and error. The values were assigned to the numerically simulated model under compression. This was done to calibrate the model based on the macro-parameter determined by the physical experiments, which are the tensile strength, Young's modulus, Poisson's ratio, and compressive strength.

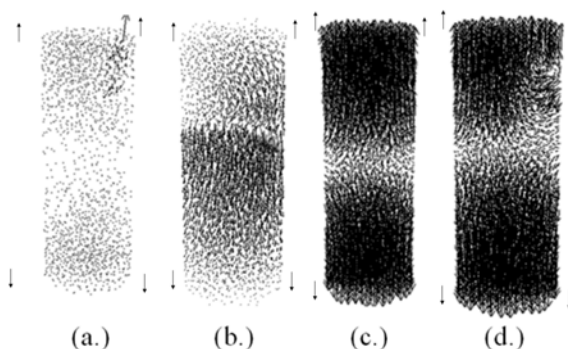


Fig. 6. Initial tension in the grain contact at velocity (a) 0.217e-8m/s (b) 0.817e-7m/s (c) 0.217e-7m (d) 4.217e-6m/s

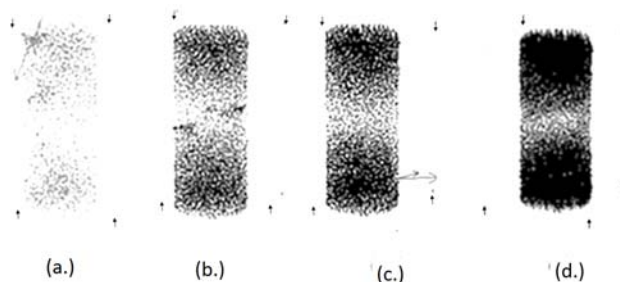


Fig. 7. Compression in the grain contact at particles displacement (a) 1.447e-7m (b) 4.217e-7m (c) 8.217e-7m (d) 10.217e-7m

Similarly, standard test were conducted and the test included the same model dimensions for both the physical and numerical experiment. The macro-parameter values of the two tests were in agreement and the tension and compression contact behavior is provided in Fig. 6 and 7 respectively with a cylindrical sample of 38 by 98mm, the stiffness ratio is 2.4. The images shows the stress transmissions though the grain assembly. This is an indication that the micro measurement is substantiated.

The redistribution of stress pattern occurs when sandstone is under stress. The attempt here seeks to validate mathematical model of a natural rock. It is known that the model validation is usually limited because findings available for evaluation are usually limited. Therefore, no single research work has exhaustively validated a natural system which means that the knowledge of the behavior of natural system is yet to be fully understood. Here, the experimental stress pattern is used to corroborate the result

from simulations. Since the observation of experimental stress pattern (Fig. 2) agrees with the natural model. The simulated model therefore is a representation of the physical system. Evidently micro-crack formation is mainly responsible for the mechanical damage of the rock model. [19], [20], [21] and [22].

IV. CONCLUSION

Some previous work have shown similarity in the quantitative contact parameter obtained in this work, (contact normal stiffness, shear stiffness as well as bond modulus), therefore the mechanical behavior of rock is largely dependent on micro mechanical properties.

The experiment show that the formation of compression-induced crack, perhaps forced the quartz grains in sandstone apart by axial load which causes bond restraining to exhibit tension. The tensions in the bonds observed at the point below the notch occurred during the early loading of the model. The tensional force chain was also observed in the simulation when micro-parameter extracted from the experiment was used for generating microstructural model. The force chains within the model matrix, also exhibit local tension at the angular notch edge because the grains at these points were angular. Therefore, the behavior of rock in nature via simulations can be reproduced because the force chains are attributed directly to its ability to generate compression-induced tensile crack as observed in the experiment.

The surface of the rock was coated with photo sensitive materials, this make it as a continuum surface that allow the interaction effect of the micro-cracks to reveal tensional and compressional localized points during the deformation. Noting that the localized points were points of micro defect in the rock, the shear stress contours obtained in the sandstone have micro structure with force chains within the grain matrix that reveal strain localization which can provide clue to theoretical solutions. In effect, physical processes of deformation of rock reveal the procedure of strain localization in natural rock. It can be conclude that the crack within the grain matrix of rock interact in nature when the material is stressed. This effect can also be reproduced by numerical simulations by incorporating the contact parameters observed due to the crack interactions observed in the experiments.

REFERENCES

[1] W. Kenneth Winkler. (1983). Contact Stiffness in Granular Porous Materials: Comparison between theory and experiment, geophysical research letters, vol. 10, No. 11 pp 1073-1076. Slumberger Doll research P.O.Box307 Ridgefield, CT 06877

[2] R.M. Holt, J. Kjolaas, I. Larsem, L. Li, A. Gotusso Pillitteri, and E.F. Sonstebo. (2005). Comparison between controlled laboratory experiments and discrete particle simulations of the mechanical behaviour of rock, International Journal of Rock Mechanics and Mining Sciences, 42(7-8): 985-995

[3] Li, I. (2012). a constitutive contact law for discrete element modelling of sandstone, Tylor and Francis Group, London. ISBN 97-0-415-80444-8 . SNTESF, petroleum research Trondheim, Norway <http://www.earthdoc.org/publication/publicationdetails/?publication=59156>

[4] Z. T., Bieniawski, C.P.G. Van Tonder. (1969). A photoelastic-model study of stress distribution and rock fracture around mining

excavations. Experimental Mechanics 9, 75–81. <https://doi.org/10.1007/BF02326677>.

[5] D.O. Potyondy and P.A. Cundall. (2004). A bonded-particle model for rock. International journal of rock mechanics and mining sciences, 41(8), 1329-1364.

[6] PA Cundall, ODL Strack. (1979). A discrete numerical model for granular assemblies. Geotechnique 29:49–65

[7] S. J. Antony, A. Olugbenga, & N. G. Ozerkan. (2018). Sensing, measuring and modelling the mechanical properties of sandstone. Rock Mechanics and Rock Engineering, 51(2), 451-464.

[8] J. H. Hanson, & A. R. Ingraffea, (1997). Standards for fracture toughness testing of rock and manufactured ceramics: what can we learn for concrete?. Cement, concrete and aggregates, 19(2), 103-111.

[9] H. Li, H. Ma, X. Shi, et al. (2020). A 3D Grain-Based Model for Simulating the Micromechanical Behavior of Salt Rock. Rock Mech Rock Eng 53, 2819–2837. <https://doi.org/10.1007/s00603-020-02085-4>.

[10] K, Senetakis and M.R. Coop. (2015). Micro-mechanical Experimental Investigation of Grain-to-Grain Sliding Stiffness of Quartz Minerals. Exp Mech 55, 1187–1190. <https://doi.org/10.1007/s11340-015-0006-4>

[11] D. A. Stow. (2005). "Sedimentary Rocks in the Field: A color guide". Gulf Professional Publishing.

[12] F. J. Pettijohn, P. E. Potter, & R. Siever. (2012). Sand and sandstone. Springer Science & Business Media.

[13] S. Boggs Jr. (2014). Principles of sedimentology and stratigraphy. Pearson Education.

[14] F. Bryant. (1958). "Snell's Law of Refraction". Physics Bulletin. 9(12), p317.

[15] D.C. Jiles. (2007). "Introduction to the principles of materials evaluation". Pg 140. CRC Press

[16] D. V. Ellis, J.M. Singer. (2007). Acoustic Waves in Porous Rocks and Boreholes. In: Ellis D.V., Singer J.M. (eds) Well Logging for Earth Scientists. Springer, Dordrecht. https://doi.org/10.1007/978-1-4020-4602-5_18.

[17] S. K. Upadhyay. (2013). "Seismic reflection processing: with special reference to anisotropy". Springer Science & Business Media.

[18] S. Van Baars. (1996), "Discrete element analysis of granular materials", Ph.D. Dissertation, Delft University, Netherlands.

[19] L. S. Costin. (2012). A micro-crack model for the deformation and failure of brittle rock, Journal of Geophysical Research: Solid Earth (1978–2012) Volume 88, Issue B11, pages 9485–9492, 10 November 1983, DOI: 10.1029/JB088iB11p09485.

[20] E. Eberhardt, D. Stead, B. Stimpson, & R. S. Read. (1997). Changes in acoustic event properties with progressive fracture damage. International Journal of Rock Mechanics and Mining Sciences, 34(3-4), 71-e1.

[21] H. Yoshida, Y. Itoyama, & H. Horii. (1999). Coupling analysis of deformation and flow in jointed rock mass during cavern excavation. Journal of applied mechanics, 2, 325-334.

[22] N. Oreskes, K. Shrader-Frechette, & K. Belitz. (1994). Verification, validation, and confirmation of numerical models in the earth sciences. Science, 263(5147), 641-646.